Neuro-Oncology
25(7), 1323–1330, 2023 | https://doi.org/10.1093/neuonc/noad029 | Advance Access date 3 February 2023

Whole-brain radiotherapy associated with structural changes resembling aging as determined by anatomic surface-based deep learning

Nikhil Rammohan, Alexander Ho, Pierre Besson, Tim J. Kruser, S. Kathleen Bandt

All author affiliations are listed at the end of the article

Corresponding Author: Nikhil Rammohan, MD, PhD, 251 E Huron St, Ste LC-178, Chicago, IL 60611, USA (nikhil-rammohan@northwestern.edu).

Abstract

Background: Brain metastases are the most common intracranial tumors in adults and are associated with significant morbidity and mortality. Whole-brain radiotherapy (WBRT) is used frequently in patients for palliation, but can result in neurocognitive deficits. While dose-dependent injury to individual areas such as the hippocampus has been demonstrated, global structural shape changes after WBRT remain to be studied.

Methods: We studied healthy controls and patients with brain metastases and examined MRI brain anatomic surface data before and after WBRT. We implemented a validated graph convolutional neural network model to estimate patient's "brain age". We further developed a mixed-effects linear model to compare the estimated age of the whole brain and substructures before and after WBRT.

Results: 4220 subjects were analyzed (4148 healthy controls and 72 patients). The median radiation dose was 30 Gy (range 25–37.5 Gy). The whole brain and substructures underwent structural change resembling rapid aging in radiated patients compared to healthy controls; the whole brain "aged" 9.32 times faster, the cortex 8.05 times faster, the subcortical structures 12.57 times faster, and the hippocampus 10.14 times faster. In a subset analysis, the hippocampus "aged" 8.88 times faster in patients after conventional WBRT versus after hippocampal avoidance (HA)-WBRT.

Conclusions: Our findings suggest that WBRT causes the brain and its substructures to undergo structural changes at a pace up to 13x of the normal aging pace, where hippocampal avoidance offers focal structural protection. Correlating these structural imaging changes with neurocognitive outcomes following WBRT or HA-WBRT would benefit from future analysis.

Key Points

- Whole-brain radiotherapy is associated with rapid structural brain "aging" compared to a normal aging pace
- Hippocampal avoidance offers focal structural protection

Brain metastases are the most common intracranial tumors in adults and are associated with significant morbidity and mortality.[1–3] In the modern era, with improvement in local and systemic therapies, patients with brain metastases are living longer; per the most recent Graded Prognostic Assessment scale, median survival for patients with ≥5 metastases, good performance status, limited extracranial disease and targetable histology is around 3–4 years.[4] Therefore, the use of WBRT has declined in favor of stereotactic radiosurgery (SRS) for the treatment of 1–4 brain metastases due to the favorable neurocognitive profile and equivalent survival following SRS compared to WBRT.[5–7] Unfortunately, many patients with brain metastases are not SRS candidates including those with leptomeningeal disease and/or numerous metastases. WBRT, therefore, remains a widely utilized treatment modality for palliation despite its known cognitive sequelae.

The decline in neurocognitive function (NCF) following WBRT is associated with a variety of deficits, including impacts

Importance of the Study

Whole-brain radiation therapy (WBRT) remains an integral part of the management of brain metastases. Unfortunately, radiation-related neurocognitive decline is a well-recognized sequela of brain radiotherapy. We utilized anatomic surface-based deep learning to examine how WBRT impacts the brain's apparent aging process via a graph convolutional neural network approach. We demonstrated that the whole brain, cortex and individual subcortical structures "aged" 6–13 times faster after WBRT compared to healthy controls. We further showed that hippocampal-avoidance WBRT offers focal structural protection. This work suggests that rapid, global structural changes analogous to aging may be a hitherto unexplored correlate of post-treatment neurocognitive deficits.

on memory, problem-solving and executive function.[6] The role of the hippocampus in memory function has been recognized for several decades.[8,9] Recent studies have demonstrated that the cognitive decline after radiation therapy was related to hippocampal injury in a dose-dependent relationship.[10,11] Based on this, hippocampal avoidance-WBRT (HA-WBRT) was developed[12]; a recent phase III randomized trial comparing HA-WBRT with the NMDA antagonist memantine versus standard WBRT and memantine (NRG-CC001) demonstrated that HA-WBRT with concurrent memantine better preserves cognitive function with no difference in survival.[13]

Cortical changes have previously been observed after intracranial radiotherapy.[14] For example, cortical volume loss can also result from targeted brain radiotherapy as is delivered in the treatment of gliomas. This can occur in a dose-dependent manner with differing regional sensitivity, and can significantly affect NCF.[15]

Our group previously developed a surface-based deep learning (SBDL) model based on anatomic brain surface morphology from high-resolution MRI to accurately predict age (error of 4.58 years) and sex (87.99% accuracy) among 6410 healthy subjects.[16] Aging is known to effect a dynamic alteration in brain shape[17]; given this, we sought to examine the effects of WBRT in relation to the pace of apparent brain aging. We hypothesized that WBRT would cause accelerated structural changes resembling aging.

Materials and Methods

High-resolution T_1-weighted MRI images from healthy controls (HC) were gathered from several publicly available repositories, which are described in detail in Supplementary Table S1. To assess the apparent aging pace, images from two scans for each subject separated by approximately 1 year were studied.

For the patient cohort, individuals aged ≥30 years who underwent WBRT at Northwestern Memorial Hospital between 2010 and 2021 for whom MRIs were available were examined. All patients with pre-treatment MRI as well as at least one follow-up MRI at least 4 weeks after treatment completion were included. Patients were selected regardless of primary histology or type of WBRT, i.e. conventional 2-field WBRT (c-WBRT) or HA-WBRT. Patients who underwent surgical resection or SRS in the post-treatment scan interval were excluded. All included patients had stable or improved disease post-treatment as determined by RANO-BM criteria.[18] Patient data were accessed with the approval of the Institutional Review Board. Supplementary Figure S1 depicts the CONSORT diagram of patient selection for the study.

The surface-based deep learning (SBDL) analysis has been described in greater detail in other publications,[16,19,20] and is only briefly summarized here. Images were processed as follows: 1) extraction of inner and outer cortical surfaces using Freesurfer (Cambridge, MA); 2) extraction of surface meshes from seven subcortical surfaces (nucleus accumbens, amygdala, caudate, hippocampus, pallidum, putamen and thalamus) using in-house written pipelines[19,20]; 3) rigid surface registration of the cortical and subcortical surfaces to the corresponding surface template[19,20]; 4) quality assessment; and 5) conversion of the surface meshes to graphs. Cortical and subcortical surfaces were visually inspected to assess their quality and ensure they accurately depict each brain's gross anatomy, and surfaces of poor quality were manually edited in a blinded fashion by P.B. and S.K.B. following Freesurfer guidelines. The final step converts the cortical and subcortical surfaces into graphs to provide input for our pre-trained graph-convolutional neural network (gCNN) toward brain age prediction at each timepoint[17] (Figure 1).

The output of the SBDL pipeline above is a model-predicted brain age for each subject ($\mathrm{Age}_i^{Pred,t}$) at a given time point *t*. To estimate aging pace between baseline (BL) and follow-up (FU) we applied a generalized linear model to each subject *i* as follows:

$$\Delta_i^{Age} = c + \psi(\Delta_i^{Scan}) + (1|\ subject)$$

where $\Delta_i^{Age} = \left(\mathrm{Age}_i^{Pred,FU} - \mathrm{Age}_i^{Actual,FU}\right) - \left(\mathrm{Age}_i^{Pred,BL} - \mathrm{Age}_i^{Actual,BL}\right)$; $\Delta_i^{Scan} = \left(\mathrm{Date}_i^{FU} - \mathrm{Date}_i^{BL}\right)$; ψ = estimated aging coefficient for group (healthy control vs WBRT); c = intercept; and $(1|\ subject)$ represents the mixed-effect term where intercept is allowed to vary per subject. In this model, $\psi = 1$ indicated no difference in estimated age between the groups, whereas $\psi > 1$ indicated WBRT patients "aged" ψ-*times* faster compared to healthy controls.

Among WBRT patients, we conducted further subgroup analyses as follows: c-WBRT vs. HA-WBRT; steroid use vs. no steroid use; memantine use vs. no memantine use. Towards these analyses, we applied another generalized linear model as follows:

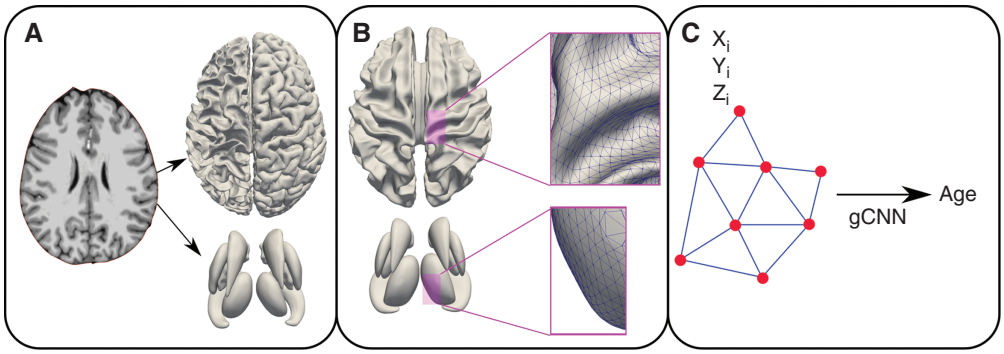

Figure 1: Surface-based deep learning pipeline. (A) Outer cortical, inner cortical and individual subcortical surfaces were extracted from T_1weighted MR image using Freesurfer. (B) Surface meshes converted to graphs using their triangulations. (C) Pre-trained graph-convolutional neural network (gCNN) predicts brain age using surface nodes' Cartesian coordinates (X, Y, Z).

$$\Delta_i^{Age} = \varphi + (1|\ subject);$$

where $\Delta_i^{Age} = \left(\text{Age}_i^{Pred,FU} - \text{Age}_i^{Actual,FU}\right)$; φ = estimated aging coefficient for subgroup (type of WBRT, Steroid Use, Memantine Use); and $(1|\ subject)$ represents the fixed-effect term.

To assess whether healthy subjects without any intracranial metastases were appropriate for comparison as a control group, we compared the estimated aging pace of a small pilot cohort (n = 15) of patients with brain metastases who underwent SRS only against our healthy cohort. We applied a generalized linear model to each subject i as follows:

$$\Delta_i^{Age} = c + \Omega(\Delta_i^{Scan}) + (1|\ subject)$$

where $\Delta_i^{Age} = \left(\text{Age}_i^{Pred,FU} - \text{Age}_i^{Actual,FU}\right) - \left(\text{Age}_i^{Pred,BL} - \text{Age}_i^{Actual,BL}\right)$; $\Delta_i^{Scan} = \left(\text{Date}_i^{FU} - \text{Date}_i^{BL}\right)$; Ω = estimated aging coefficient for group (healthy control vs SRS); c = intercept; and $(1|\ subject)$ represents the mixed-effect term where intercept is allowed to vary per subject. In this model, $\Omega = 1$ indicated no difference in estimated age between the groups, whereas $\Omega > 1$ indicated SRS patients "aged" Ω -times faster compared to healthy controls.

To compare estimated aging pace between groups with several brain substructures, the Bonferroni method was utilized to correct for multiple comparisons.

Results

Patient characteristics are shown in Table 1. 4148 healthy controls and 72 WBRT patients were studied. The median age was 74 years (range 42–95 years) for the control group and 62 years (range 32–85 years) for the WBRT group. WBRT patients were predominantly female, with good performance status (86% KPS ≥ 70), predominantly with breast and lung primary tumors, and the majority (79%) had ≥5 metastases. Median WBRT dose was 30Gy (range 25–37.5 Gy). Median interscan interval was 12.0 months for the healthy controls and 6.2 months for the WBRT group. The majority of patients (66%) did not have intracranial-directed treatment (surgical resection or SRS) prior to WBRT. The majority of patients (81%) had systemic therapy prior to WBRT and all patients had systemic therapy post-WBRT; Table S2 demonstrates the type of chemotherapy received by the WBRT patients. 71% of WBRT patients were given memantine and 57% were given steroids concurrently. For the SRS patient cohort, the median age was 62.5 years; 64% were female; 79% comprised breast or lung primaries; median number of brain metastases = 5 (range 2-8); all patients received 20 Gy in single fraction Gamma Knife SRS; 57% received prior systemic therapy; 100% received post-treatment systemic therapy; median follow up was 5.8 months; patients with prior resection or WBRT, or resection/SRS/WBRT in the follow up period were excluded.

We compared apparent aging pace between the healthy controls and WBRT patients in Table 2. The whole brain, cortex and all individual subcortical structures "aged" more rapidly after WBRT compared to healthy controls (ψ >> 1). Since ψ represents the estimated aging coefficient, we demonstrated that after WBRT, the whole brain "aged" 9.32 times faster, the cortex 8.04 times faster, the subcortical structures combined 12.57 times faster, and the hippocampus 10.14 times faster, compared to healthy controls. The intercept term c provides an estimate of Δ^{Age} between healthy controls and WBRT patients pre-treatment; since $c \approx 0$ for whole brain, cortex and all subcortical structures, we concluded pre-treatment Δ^{Age} is not significantly different between the groups. A spaghetti plot comparing slopes of *whole brain* estimated aging of healthy controls versus WBRT patients is shown in Figure 2. The estimated aging slope of WBRT patients is significantly steeper than healthy control group. We depict similar spaghetti plots of comparative aging pace of the cortex, combined subcortical structures and the hippocampus in Supplementary Figures S2-S4, all of which show apparent rapid aging after WBRT compared to healthy controls. We acknowledge that comparison against a healthy cohort with no history of malignancy may not be ideal. We therefore identified a small pilot cohort of patients with brain metastases who

Table 1. Patient Characteristics

	Controls	WBRT
Variable	Number (%)	Number (%)
N	4148	72
Age (years)		
Median	73	62
Range	42 – 95	32 - 85
Sex		
Male	1929	20 (28)
Female	2219	52 (72)
Karnofsky Performance Status		
90–100	n/a	30 (42)
70–80		33 (46)
<70		9 (12)
# Brain metastases		
0	n/a	2 (3)
1–4		14 (19)
≥5		57 (79)
Organ Site		
Breast	n/a	32 (44)
Lung		30 (42)
Other		11 (15)
WBRT dose (Gy)		
Median	n/a	30
Range		25 – 37.5
Median follow up (months)	12.0	6.2
Prior Resection	n/a	
Yes		4 (6)
No		68 (94)
Prior SRS	n/a	
Yes		17 (18)
No		55 (82)
Prior systemic therapy	n/a	
Yes		58 (81)
No		14 (19)
Post-WBRT systemic therapy	n/a	
Yes		72 (100)
No		0 (0)
Concurrent memantine	n/a	
Yes		16 (29)
No		40 (71)
Steroid use	n/a	
Yes		24 (43)
No		32 (57)

underwent SRS only and we compared the estimated aging pace against healthy controls (Table S3); we showed that the estimated aging pace of SRS patients was not significantly different from healthy subjects suggesting that the latter group is meaningful for comparison.

Among the WBRT patients, we assessed apparent aging pace of whole brain, cortex, and subcortical structures among several subgroups. First, we compared estimated aging pace among patients who underwent HA-WBRT (17 patients) vs. c-WBRT (55 patients); φ >1 indicated that

Table 2. SBDL model comparing estimated aging pace between healthy controls and WBRT patients. $\psi > 1$ indicated WBRT patients "aged" ψ-times faster than healthy controls. Intercept *c* serves as surrogate for pre-treatment difference in Δ^{Age} between WBRT patients and healthy controls. *Bonferroni cutoff $p < 0.005$ for uncorrected p-values.

Structure	ψ (95% CI)	*c* (95% CI)	Uncorrected *p*-value*
Whole Brain	**9.32** (8.09, 10.56)	–0.079 (–0.209, 0.051)	<0.001
Cortex	**8.05** (6.90, 9.21)	0.077 (–0.046, 0.200)	<0.001
Subcortical	**12.57** (10.77, 14.36)	–0.016 (–0.208, 0.176)	<0.001
Nucleus Accumbens	**8.69** (7.20, 10.18)	–0.072 (–0.238, 0.095)	<0.001
Amygdala	**6.43** (4.94, 7.92)	–0.037 (–0.192, 0.119)	<0.001
Caudate	**7.84** (6.55, 9.14)	–0.075 (–0.214, 0.064)	<0.001
Hippocampus	**10.15** (8.55, 11.75)	0.021 (–0.154, 0.196)	<0.001
Pallidum	**8.64** (7.11, 10.17)	0.015 (–0.153, 0.182)	<0.001
Putamen	**9.65** (8.01, 11.28)	0.037 (–0.137, 0.211)	<0.001
Thalamus	**7.59** (5.87, 9.30)	0.237 (0.058, 0.417)	<0.001

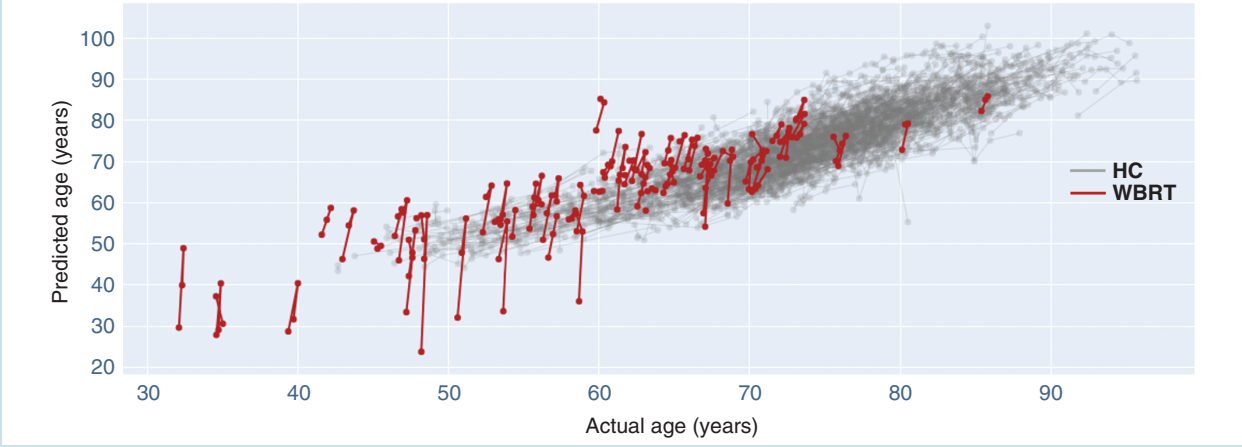

Figure 2: Spaghetti plot of *whole brain* "aging" over time for healthy controls (HC) vs. WBRT patients. Estimated aging slope of WBRT patients significantly steeper than best-fit aging slope of healthy controls.

Table 3. Estimated aging pace comparison between patients who underwent c-WBRT vs HA-WBRT. $\varphi > 1$ indicated c-WBRT patients "aged" faster compared to HA-WBRT patients and non-significant φ indicated no difference in Δ^{Age} between groups. *Bonferroni cutoff $p < 0.005$ for uncorrected p-values.

Structure	φ (95% CI)	Uncorrected p-value
Whole Brain	**–0.674** (–4.36, 3.02)	0.720
Cortex	**–3.40** (–6.91, 0.114)	0.058
Subcortical	**1.77** (–3.02, 6.56)	0.468
Nucleus Accumbens	**0.731** (–3.24, 4.70)	0.718
Amygdala	**2.34** (–0.921, 5.59)	0.160
Caudate	**–2.15** (–6.12, 1.82)	0.288
Hippocampus	***8.83**** *(3.63, 14.0)*	***0.001****
Pallidum	**–0.353** (–4.34, 3.63)	0.862
Putamen	**5.49** (0.721, 10.3)	0.02
Thalamus	**6.28** (–0.004, 10.7)	0.042

c-WBRT patients "aged" faster that HA-WBRT patients and non-significant φ indicated no difference in Δ^{Age} between c-WBRT and HA-WBRT patients. In Table 3, we demonstrate that the hippocampus "aged" 8.83 times faster in the c-WBRT group compared to the HA-WBRT (φ = 8.83, p = 0.01 Bonferroni corrected) while the whole brain, cortex and other subcortical structures were not significantly different (Bonferroni cutoff $p < 0.005$ for uncorrected p-values). Further subgroup analyses for steroid use vs. no steroid use (Supplementary Table S4), and memantine use vs. no memantine use (Supplementary Table S5) demonstrated no significant differences in Δ^{Age}.

Discussion

While cortical *volume* changes after WBRT have been previously described,[21] findings from these investigations are the first to demonstrate – to the best of our knowledge – that WBRT is associated with rapid, global, measurable structural *shape* changes that parallel those seen in the aging brain (Table 2, Figure 2). These changes could potentially explain the neurocognitive deficits seen after treatment. Numerous investigators have shown previously that accelerated aging processes measured by similar surface morphometry techniques are associated with neurocognitive dysfunction in other pathologic processes such as Alzheimer disease and other forms of dementia.[22–26] The nature of our study cohort led to a relatively abbreviated median follow-up duration of 6.2 months. Given that the effects of WBRT can linger months to years after treatment,[27] it is possible that with longer-term follow up, continued further apparent accelerated brain aging may be identified in this population.

Furthermore, we show that HA-WBRT results in focal sparing of the hippocampus in terms of apparent aging pace (Table 3), which is congruent with the maintained neurocognitive profile seen in these patients.[12,13] Memory loss related to structural changes including volume loss affecting the hippocampus in normal aging and dementias is well-studied.[22,26,28,29] Structural changes defined herein following c-WBRT are consistent with these other etiologies of cognitive impairment. Interestingly, the estimated aging pace of the whole brain, cortex and other subcortical structures are not significantly different between patients who underwent HA-WBRT versus c-WBRT (Table 3); this suggests that while the hippocampus may be focally spared, the rest of the brain still "ages" rapidly compared to healthy controls. Along those lines, several cooperative group multi-institutional trials, including NRG CC009, CCTG CE.7, and NRG BN009, are evaluating extra-hippocampal structural changes when comparing HA-WBRT with SRS; additionally these concepts are also of interest in pediatric neuro-oncology trials (e.g. curative-intent craniospinal irradiation).

Cognitive dysfunction after systemic therapy, often termed "chemo brain,"[30–33] has been associated with long term chemotherapy and immunotherapy, and all WBRT patients in our study also received some form of systemic therapy in the post-treatment scan interval (see Supplementary Table S2). Therefore, we recognize the challenge of attributing all post-treatment brain changes to WBRT alone. However, there are some factors that allude to WBRT playing a specific role in the aging phenomenon we demonstrate. Firstly, "BL" scans were not significantly different in Δ^{Age} between groups (Table 2), where a majority of WBRT patients (81%) had some form of systemic therapy prior to WBRT (Table 1, Supplementary Table S2). Secondly, the structural protection conferred to the hippocampus in HA-WBRT patients (Table 3) who all underwent post-WBRT systemic therapy also show that the effects of radiation are easily detectable. Finally, even though steroids and memantine have been shown to alleviate the neurocognitive side-effects of WBRT, these interventions did not have significant impact on Δ^{Age}, suggesting that structural changes after WBRT may be dichotomous from inflammatory and biochemical changes that can be intervened upon.

Overall, given patients are living longer with brain metastases, consideration for patient quality of life have become significantly more important.[4,34] Since WBRT is associated with rapid apparent aging, our results further indicate that c-WBRT should be used sparingly, such as for extensive burden of disease or neurologic compromise where other intracranial-directed therapies are not possible.[35] Our results also have implications for situations where WBRT has historically been standard-of-care, such as been the case for brain metastases in the setting of SCLC. A recent meta-analysis by Gaebe et al.[36] indicate similar survival outcomes between SRS and WBRT for patients with brain metastases secondary to SCLC. Further, with regard to prophylactic cranial irradiation (PCI) in limited-stage SCLC, a recent study demonstrated that PCI with WBRT demonstrated little survival benefit.[37] HA-WBRT has shown promise in preserving neurocognitive function compared to c-WBRT, and there are several ongoing prospective multi-institutional randomized trials comparing HA-WBRT and SRS in terms of disease control and neurocognitive outcomes.

The authors recognize limitations in our study. Firstly, we concede this is a retrospective analysis and our conclusions are guarded given absence of prospective validation or correlation with neurocognitive outcomes. Furthermore, given patients were required to have adequate follow up with MRI, the WBRT cohort sample size was small, where many patients who were treated palliatively without follow up or had died soon after treatment were unable to be studied. In this context, a future larger prospective study is warranted. Secondly, the SBDL pipeline was developed to study aging in healthy patients, so there may be limited external validity when applied to diseased brains. However, the SBDL algorithm was also inherently designed to be robust to a relatively heterogeneous image cohort, given the vastly different image acquisition parameters between institutions in the repositories. Along these lines, as referenced earlier, "BL" scan between groups were not significantly different in Δ^{Age} demonstrating that age prediction remained as effective in the WBRT cohort as in the healthy cohort. Lastly, our pilot SRS cohort comprised only 15 patients; a direct and robust comparison between SRS and WBRT with larger sample sizes are required in the future.

In conclusion, with the WBRT-mediated apparent accelerated aging shown herein, we add to the growing cluster of studies that re-examine the role of WBRT in the modern era. Further work investigating the differential impact on apparent brain aging and cognition between c-WBRT, HA-WBRT and SRS are ongoing.

Supplementary Material

Supplementary material is available online at *Neuro-Oncology* (http://neuro-oncology.oxfordjournals.org/).

Keywords

brain metastases | MRI | deep learning | aging

Acknowledgements

The authors thank the Northwestern Medicine Quest High Performance Computing Cluster.

Funding

This work was supported by the Northwestern University P50CA221747 SPORE for Translational Approaches to Brain Cancer

Conflict of Interest Statement

TJK serves on an advisory board and speakers bureau for AstraZeneca and is a consultant for Radialogica LLC. Other authors declare they have no conflicts of interest.

Authorship Statement

Project ideas and methods: N.R., P.B., T.J.K and S.K.B; Data curation: N.R., A.H.; Data analysis: N.R., A.H., P.B.; Writing (first draft and revisions): N.R., A.H.; Writing (editing): P.B., T.J.K., S.K.B.

Affiliations

Department of Radiation Oncology, Northwestern University Feinberg School of Medicine, Chicago, IL, USA (N.R. A. H.); Department of Radiology, Northwestern University Feinberg School of Medicine, Chicago, IL, USA (P. B.); SSM Health Dean Medical Group, Turville Bay Radiation Oncology Center, Madison, WI, USA (T. J. K.); Department of Neurologic Surgery, Northwestern University Feinberg School of Medicine, Chicago, IL, USA (S. K. B.)

References

1. Brown PD, Ahluwalia MS, Khan OH, et al. Whole-brain radiotherapy for brain metastases: evolution or revolution? *J Clin Oncol.* 2018;36(5):483–491.
2. Brown PD. Whole brain radiotherapy for brain metastases. *BMJ* 2016;355:i6483.
3. Khuntia D, Brown P, Li J, Mehta MP. Whole-brain radiotherapy in the management of brain metastasis. *J Clin Oncol.* 2006;24(8):1295–1304.
4. Sperduto PW, Mesko S, Li J, et al. Survival in patients with brain metastases: summary report on the updated diagnosis-specific graded prognostic assessment and definition of the eligibility quotient. *J Clin Oncol.* 2020;38(32):3773–3784.
5. Brown PD, Ballman KV, Cerhan JH, et al. Postoperative stereotactic radiosurgery compared with whole brain radiotherapy for resected metastatic brain disease (NCCTG N107C/CEC.3): a multicentre, randomised, controlled, phase 3 trial. *Lancet Oncol.* 2017;18(8):1049–1060.
6. Brown PD, Jaeckle K, Ballman KV, et al. Effect of radiosurgery alone vs radiosurgery with whole brain radiation therapy on cognitive function in patients with 1 to 3 brain metastases: a randomized clinical trial. *JAMA.* 2016;316(4):401–409.
7. Aoyama H, Tago M, Shirato H. Stereotactic Radiosurgery With or Without Whole-Brain Radiotherapy for Brain Metastases: Secondary Analysis of the JROSG 99-1 Randomized Clinical Trial. *JAMA Oncol* 2015;1(4):457–464.
8. Gondi V, Paulus R, Bruner DW, et al. Decline in tested and self-reported cognitive functioning after prophylactic cranial irradiation for lung cancer: pooled secondary analysis of Radiation Therapy Oncology Group randomized trials 0212 and 0214. *Int J Radiat Oncol Biol Phys.* 2013;86(4):656–664.
9. Gondi V, Tome WA, Mehta MP. Why avoid the hippocampus? A comprehensive review. *Radiother Oncol.* 2010;97(3):370–376.
10. Leung SF, Kreel L, Tsao SY. Asymptomatic temporal lobe injury after radiotherapy for nasopharyngeal carcinoma: incidence and determinants. *Br J Radiol.* 1992;65(776):710–714.
11. Abayomi OK. Pathogenesis of irradiation-induced cognitive dysfunction. *Acta Oncol.* 1996;35(6):659–663.
12. Gondi V, Pugh SL, Tome WA, et al. Preservation of memory with conformal avoidance of the hippocampal neural stem-cell compartment during whole-brain radiotherapy for brain metastases (RTOG 0933): a phase II multi-institutional trial. *J Clin Oncol.* 2014;32(34):3810–3816.
13. Brown PD, Gondi V, Pugh S, et al. Hippocampal avoidance during whole-brain radiotherapy plus memantine for patients with brain metastases: phase III trial NRG oncology CC001. *J Clin Oncol.* 2020;38(10):1019–1029.
14. Nagtegaal SHJ, David S, van der Boog ATJ, Leemans A, Verhoeff JJC. Changes in cortical thickness and volume after cranial radiation treatment: A systematic review. *Radiother Oncol.* 2019;135:33–42.
15. Karunamuni R, Bartsch H, White NS, et al. Dose-dependent cortical thinning after partial brain irradiation in high-grade glioma. *Int J Radiat Oncol Biol Phys.* 2016;94(2):297–304.
16. Besson P, Parrish T, Katsaggelos AK, Bandt SK. Geometric deep learning on brain shape predicts sex and age. *Comput Med Imaging Graph.* 2021;91:101939.

17. Besson P, Rogalski E, Gill NP, et al. Geometric deep learning reveals a structuro-temporal understanding of healthy and pathologic brain aging. *Front Aging Neurosci.* 2022;14:895535.
18. Lin NU, Lee EQ, Aoyama H, et al. Response assessment criteria for brain metastases: proposal from the RANO group. *Lancet Oncol.* 2015;16(6):e270–e278.
19. Besson P, Carriere N, Bandt SK, et al. Whole-brain high-resolution structural connectome: inter-subject validation and application to the anatomical segmentation of the striatum. *Brain Topogr.* 2017;30(3):291–302.
20. Besson P, Lopes R, Leclerc X, Derambure P, Tyvaert L. Intra-subject reliability of the high-resolution whole-brain structural connectome. *Neuroimage.* 2014;102(Pt 2):283–293.
21. Hoffmann C, Distel L, Knippen S, et al. Brain volume reduction after whole-brain radiotherapy: quantification and prognostic relevance. *Neuro Oncol* 2018;20(2):268–278.
22. Miller MI, Priebe CE, Qiu A, et al. Collaborative computational anatomy: an MRI morphometry study of the human brain via diffeomorphic metric mapping. *Hum Brain Mapp.* 2009;30(7):2132–2141.
23. Miller MI, Hosakere M, Barker AR, et al. Labeled cortical mantle distance maps of the cingulate quantify differences between dementia of the Alzheimer type and healthy aging. *Proc Natl Acad Sci U S A.* 2003;100(25):15172–15177.
24. Azcona E, Besson P, Wu Y, et al. Interpretation of Brain Morphology in Association to Alzheimer's Disease Dementia Classification Using Graph Convolutional Networks on Triangulated Meshes. *Shape Med Imaging (2020)* 2020;12474:95–107.
25. Creze M, Versheure L, Besson P, et al. Age- and gender-related regional variations of human brain cortical thickness, complexity, and gradient in the third decade. *Hum Brain Mapp.* 2014;35(6):2817–2835.
26. Kim H, Besson P, Colliot O, Bernasconi A, Bernasconi N. Surface-based vector analysis using heat equation interpolation: a new approach to quantify local hippocampal volume changes. *Med Image Comput Comput Assist Interv.* 2008;11(Pt 1):1008–1015.
27. Tallet AV, Azria D, Barlesi F, et al. Neurocognitive function impairment after whole brain radiotherapy for brain metastases: actual assessment. *Radiat Oncol.* 2012;7:77.
28. Zhang J, Xu D, Cui H, et al. Group-guided individual functional parcellation of the hippocampus and application to normal aging. *Hum Brain Mapp.* 2021;42(18):5973–5984.
29. Profant O, Skoch A, Tintera J, et al. The influence of aging, hearing, and tinnitus on the morphology of cortical gray matter, amygdala, and hippocampus. *Front Aging Neurosci.* 2020;12:553461.
30. Hermelink K. Chemotherapy and cognitive function in breast cancer patients: the so-called chemo brain. *J Natl Cancer Inst Monogr.* 2015;2015(51):67–69.
31. Hermelink K, Untch M, Lux MP, et al. Cognitive function during neoadjuvant chemotherapy for breast cancer: results of a prospective, multicenter, longitudinal study. *Cancer.* 2007;109(9):1905–1913.
32. Staat K, Segatore M. The phenomenon of chemo brain. *Clin J Oncol Nurs.* 2005;9(6):713–721.
33. Joly F, Castel H, Tron L, Lange M, Vardy J. Potential effect of immunotherapy agents on cognitive function in cancer patients. *J Natl Cancer Inst.* 2020;112(2):123–127.
34. Steinmann D, Paelecke-Habermann Y, Geinitz H, et al. Prospective evaluation of quality of life effects in patients undergoing palliative radiotherapy for brain metastases. *BMC Cancer* 2012;12:283.
35. Vogelbaum MA, Brown PD, Messersmith H, et al. Treatment for brain metastases: ASCO-SNO-ASTRO guideline. *J Clin Oncol.* 2022;40(5):492–516.
36. Gaebe K, Li AY, Park A, et al. Stereotactic radiosurgery versus whole brain radiotherapy in patients with intracranial metastatic disease and small-cell lung cancer: a systematic review and meta-analysis. *Lancet Oncol.* 2022;23(7):931–939.
37. Pezzi TF, Gjyshi O, Feng L, et al. Rates of overall survival and intracranial control in the magnetic resonance imaging era for patients with limited-stage small cell lung cancer with and without prophylactic cranial irradiation. *JAMA Network Open* 2020;3(4):e201929.